Transport in simple networks described by an integrable discrete nonlinear Schrödinger equation

K. Nakamura,[1,2] Z. A. Sobirov,[3] D. U. Matrasulov,[3] and S. Sawada[4]
[1]*Faculty of Physics, National University of Uzbekistan, Vuzgorodok, Tashkent 100174, Uzbekistan*
[2]*Department of Applied Physics, Osaka City University, Osaka 558-8585, Japan*
[3]*Turin Polytechnic University in Tashkent, 17 Niyazov Street, Tashkent 100093, Uzbekistan*
[4]*Department of Physics, Kwansei Gakuin University, Sanda 669-1337, Japan*
(Received 17 May 2011; published 15 August 2011)

We elucidate the case in which the Ablowitz-Ladik (AL)-type discrete nonlinear Schrödinger equation (NLSE) on simple networks (e.g., star graphs and tree graphs) becomes completely integrable just as in the case of a simple one-dimensional (1D) discrete chain. The strength of cubic nonlinearity is different from bond to bond, and networks are assumed to have at least two semi-infinite bonds with one of them working as an incoming bond. The present work is a nontrivial extension of our preceding one [Sobirov *et al.*, Phys. Rev. E **81**, 066602 (2010)] on the continuum NLSE to the discrete case. We find (1) the solution on each bond is a part of the universal (bond-independent) AL soliton solution on the 1D discrete chain, but it is multiplied by the inverse of the square root of bond-dependent nonlinearity; (2) nonlinearities at individual bonds around each vertex must satisfy a sum rule; and (3) under findings 1 and 2, there exist an infinite number of constants of motion. As a practical issue, with the use of an AL soliton injected through the incoming bond, we obtain transmission probabilities inversely proportional to the strength of nonlinearity on the outgoing bonds.

DOI: 10.1103/PhysRevE.84.026609 PACS number(s): 05.45.Yv, 03.75.−b

I. INTRODUCTION

We investigate transport in networks with vertices and bonds, which has received growing attention recently. The networks of practical importance are those of nonlinear waveguides and optical fibers [1], the double helix of DNA [2], Josephson junction arrays with Bose- Einstein condensates (BECs) [3], topology-induced BECs in complex networks [4], vein networks in leaves [5,6], etc.

A major theoretical concern so far, however, is limited to solving stationary states of the linear Schrödinger equation and to obtaining the energy spectra in closed networks and transmission probabilities for open networks with semi-infinite leads [7–12]. Only a few studies treat the nonlinear Schrödinger equation on simple networks, which are still limited to the analysis of its stationary state [13,14].

With the introduction of nonlinearity to the time-dependent Schrödinger equation, the network provides a nice playground where one can see interesting soliton propagations and nonlinear dynamics through the network [15–18], namely through an assembly of continuum line segments connected at vertices. Although there exist important analytical studies on semi-infinite and finite chains [19–22], we find little exact analytical treatment of soliton propagation through networks within a nonlinear Schrödinger equation (NLSE) framework [23,24]. The subject is difficult due to the presence of vertices where the underlying chain should bifurcate or multifurcate in general.

Recently, with a suitable boundary condition at each vertex, we developed an exact analytical treatment of soliton propagation through networks within a NLSE framework [25]. Under an appropriate relationship among values of nonlinearity at individual bonds, we found nonlinear dynamics of solitons with no reflection at the vertex. We also showed that an infinite number of constants of motion are available for NLSE on networks; namely, the mapping of the Zakharov-Shabat scheme [26] to networks was achieved.

The extension of the scenario to the discrete NLSE (DNLSE) is far from being obvious. The standard DNLSE is not integrable and the integrable variant of the continuum nonlinear Schrödinger equation is the one proposed by Ablowitz and Ladik [24,27–29]. The Ablowitz-Ladik (AL) equation is the appropriate choice for the zero-order approximation in studying the soliton dynamics perturbatively in physically motivated models, such as an array of coupled optical waveguides [30] and proton dynamics in hydrogen-bonded chains [31,32]. The dynamics of intrinsic localized modes in nonlinear lattices can be approximately described by the AL equation [33]. Exciton systems with exchange and dipole-dipole interactions also reduce to the AL equation in some limiting cases [34]. The AL chain is integrable by means of the inverse scattering transform and, together with the Toda lattice [35], constitutes a paradigm of the completely integrable lattice systems.

The AL equation for a field variable ψ on a one-dimensional (1D) chain is given by

$$i\dot{\psi}_n + (\psi_{n+1} + \psi_{n-1})(1 + \gamma|\psi_n|^2) = 0, \qquad (1)$$

where γ is the strength of nonlinear intersite interaction and n denotes each lattice site on the chain. This equation can be obtained from the canonical equation of motion with use of the nonstandard Poisson brackets. Equation (1) has an infinite number of independent constants of motion and is completely integrable [27,28].

However, there is an ambiguity in generalizing the AL model to networks: how can we define the intersite interaction at each vertex in order to see the infinite number of constants of motion in networks? To keep the integrability of the AL equation, should any rule hold for the strength of nonlinearity on bonds joining at each vertex? We resolve these questions in this paper and show how solitons of the AL equation on networks are mapped to that of the AL equation on a 1D chain. Once this mapping is found, the integrability properties, such as the inverse scattering transform, the Bäcklund transformation, etc., are automatically guaranteed and are not addressed in this paper.

Below we show the completely integrable case of the AL equation on networks with strength of nonlinearity different from bond to bond. As a relevant issue, with the use of reflectionless propagation of an AL soliton through networks, we evaluate the transmission probabilities on the outgoing bonds. In Sec. II, using a primary star graph (PSG) and defining a suitable equation of motion at the vertex, we address the norm and energy conservations. In Sec. III, we show a basic idea of the soliton propagation along the branched chain, finding the connection formula at the vertex and the sum rule among the strengths of nonlinearity on the bonds, which guarantee the infinite number of constants of motion and complete integrability of the system under consideration. In Sec. IV, the cases of generalized star graphs and tree graphs are investigated. Section V is devoted to the investigation of an injection of an AL soliton which bifurcates at the vertex and is decomposed into a pair of solitons with each propagating along the outgoing bonds, and we evaluate the transmission probabilities on the outgoing bonds. Summary and discussions are given in Sec. VI.

II. NORM AND ENERGY CONSERVATIONS ON PRIMARY STAR GRAPH

A. AL equation on networks

Let us consider an elementary branched chain (see Fig. 1), namely, a PSG consisting of three semi-infinite bonds connected at the vertex O. We denote individual lattice sites as (k,n), where $k=1,2,3$ is the bond's number and n corresponds to a lattice site on each bond. For the first bond ($k=1$), n is numbered as $n \in B_1 = \{0,-1,-2,\ldots\}$, where (1, 0) means the branching point, i.e., the vertex. For the second ($k=2$) and third ($k=3$) bonds, n varies as $n \in B_k = \{1,2,3,\ldots\}$; (2,1) and (3,1) stand for the points nearest to the vertex.

A DNLSE *à la* AL is defined on each bond, except for in the vicinity of the vertex, as

$$i\dot{\psi}_{k,n} + (\psi_{k,n+1} + \psi_{k,n-1})(1+\gamma_k|\psi_{k,n}|^2) = 0, \tag{2}$$

where $(k,n) \notin \{(1,0),(2,1),(3,1)\}$. It should be noted that γ_k may be different among bonds. There is an ambiguity about

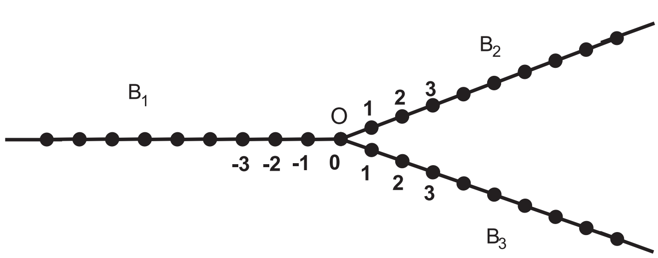

FIG. 1. Primary star graph. Three semi-infinite chains, B_1, B_2, and B_3, connected at a vertex O.

the interaction around the vertex, which is resolved as follows: Let us first introduce the Hamiltonian for a PSG as

$$H = -\sum_{n=0}^{-\infty}(\psi^*_{1,n}\psi_{1,n+1} + \text{c.c.}) - \sum_{k=2}^{3}\sum_{n=1}^{+\infty}(\psi^*_{k,n}\psi_{k,n+1} + \text{c.c.}), \tag{3}$$

where at the virtual site (1,1) we assume $\psi_{1,1} = s_2\psi_{2,1} + s_3\psi_{3,1}$ with appropriate coefficients s_2 and s_3. Then Eq. (2) can be obtained by the equation of motion

$$i\dot{\psi}_{k,n} = \{H,\psi_{k,n}\} \tag{4}$$

at $(k,n) \notin \{(1,0),(2,1),(3,1)\}$, with use of nonstandard Poisson brackets

$$\begin{aligned}\{\psi_{k,m},\psi^*_{k',n}\} &= i(1+\gamma|\psi_{k,m}|^2)\delta_{kk'}\delta_{mn},\\ \{\psi_{k,m},\psi_{k',n}\} &= \{\psi^*_{k,m},\psi^*_{k',n}\} = 0.\end{aligned} \tag{5}$$

On the same footing as above, the equations of motion in Eq. (4) at (1,0), (2,1), and (3,1) are given, respectively, as

$$i\dot{\psi}_{1,0} + (\psi_{1,-1} + s_2\psi_{2,1} + s_3\psi_{3,1})(1+\gamma_1|\psi_{1,0}|^2) = 0, \tag{6}$$

$$i\dot{\psi}_{k,1} + (s_k\psi_{1,0} + \psi_{k,2})(1+\gamma_k|\psi_{k,1}|^2) = 0,\ \ k=2,3. \tag{7}$$

The solution is assumed to satisfy the following conditions at infinity: $\psi_{1,n} \to 0$ at $n \to -\infty$ and $\psi_{k,n} \to 0$ at $n \to +\infty$ for $k=2$ and 3.

B. Norm and energy conservations

It is known that the norm conservation is one of the most important physical conditions in conservative systems. Since Eqs. (2), (6), and (7) are available from Hamilton's equation of motion with nonstandard Poisson brackets, the norm and energy conservations seem obvious. Below, however, we observe them explicitly. Extending the definition in the case of a 1D chain [24], the norm for a PSG is given as

$$N = \|\psi\|^2 = \sum_{k=1}^{3}\frac{1}{\gamma_k}\sum_{n\in B_k}\ln(1+\gamma_k|\psi_{k,n}|^2). \tag{8}$$

Its time derivative is given by

$$\frac{d}{dt}N = \sum_{k=1}^{3}\sum_{n\in B_k}A_{k,n} \tag{9}$$

with

$$A_{k,n} = \frac{1}{1+\gamma_k|\psi_{k,n}|^2}(\psi^*_{k,n}\dot{\psi}_{k,n} + \dot{\psi}^*_{k,n}\psi_{k,n}). \tag{10}$$

For $(k,n) \notin \{(1,0),(2,1),(3,1)\}$ with use of Eq. (2) we have

$$\begin{aligned}A_{k,n} &= \frac{1}{i}(\psi_{k,n}\psi^*_{k,n+1} - \psi^*_{k,n}\psi_{k,n+1})\\ &\quad - \frac{1}{i}(\psi_{k,n-1}\psi^*_{k,n} - \psi^*_{k,n-1}\psi_{k,n}) \equiv j_{k,n} - j_{k,n-1},\end{aligned} \tag{11}$$

where

$$j_{k,n} \equiv \frac{1}{i}(\psi_{k,n}\psi^*_{k,n+1} - \psi^*_{k,n}\psi_{k,n+1}) \tag{12}$$

implies a local current. First, one observes

$$\sum_k \sum_n{}' A_{k,n} = j_{1,0} - j_{2,1} - j_{3,1}, \tag{13}$$

where $\sum_k \sum_n{}'$ means the summation over all sites on a PSG except for the points (1,0), (2,1), and (3,1).

Then, for $(k,n) = (1,0),(2,1),(3,1)$, with use of Eqs. (6) and (7) we obtain

$$A_{1,0} = s_2 \frac{1}{i}(\psi_{1,0}\psi_{2,1}^* - \psi_{1,0}^*\psi_{2,1}) + s_3 \frac{1}{i}(\psi_{1,0}\psi_{3,1}^* - \psi_{1,0}^*\psi_{3,1}) - j_{1,0} \tag{14}$$

and

$$A_{k,1} = j_{k,1} - s_k \frac{1}{i}(\psi_{1,0}\psi_{k,1}^* - \psi_{1,0}^*\psi_{k,1}) \tag{15}$$

for $k = 2,3$. Substituting Eqs. (13)–(15) into Eq. (9), we can see $\frac{d}{dt}N = 0$, i.e., the norm conservation. Therefore, for any choice of values s_2 and s_3, the norm conservation turns out to hold well.

On the other hand, the energy for a PSG is expressed in a symmetrical form as

$$E = -2\mathrm{Re}\left[\sum_{n=-1}^{-\infty} \psi_{1,n}^*\psi_{1,n+1} + \sum_{k=2}^{3}\sum_{n=1}^{+\infty} \psi_{k,n}^*\psi_{k,n+1} + \psi_{1,0}^*(s_2\psi_{2,1} + s_3\psi_{3,1})\right]. \tag{16}$$

To show that the energy is conservative, we see its time derivative:

$$\begin{aligned}\frac{d}{dt}E = &-2\mathrm{Re}\sum_{n=-1}^{-\infty}(\psi_{1,n}^*\dot{\psi}_{1,n+1} + \dot{\psi}_{1,n}^*\psi_{1,n+1}) \\ &- 2\mathrm{Re}\sum_{k=2}^{3}\sum_{n=1}^{+\infty}(\psi_{k,n}^*\dot{\psi}_{k,n+1} + \dot{\psi}_{k,n}^*\psi_{k,n+1}) \\ &- 2\mathrm{Re}[\psi_{1,0}^*(s_2\dot{\psi}_{2,1} + s_3\dot{\psi}_{3,1}) \\ &+ \dot{\psi}_{1,0}^*(s_2\psi_{2,1} + s_3\psi_{3,1})].\end{aligned} \tag{17}$$

With use of Eq. (2) we have

$$\begin{aligned}&-\sum_{n=-1}^{-\infty}(\psi_{1,n}^*\dot{\psi}_{1,n+1} + \dot{\psi}_{1,n}^*\psi_{1,n+1}) \\ &= \frac{1}{i}\sum_{n=-1}^{-\infty}[|\psi_{1,n-1}|^2 - |\psi_{1,n+1}|^2] \\ &\quad\times(1 + \gamma_1|\psi_{1,n}|^2) - \psi_{1,-1}^*\dot{\psi}_{1,0},\end{aligned} \tag{18}$$

and

$$\begin{aligned}&-\sum_{n=1}^{\infty}(\psi_{k,n}^*\dot{\psi}_{k,n+1} + \dot{\psi}_{k,n}^*\psi_{k,n+1}) \\ &= \frac{1}{i}\sum_{n=2}^{\infty}[|\psi_{k,n-1}|^2 - |\psi_{k,n+1}|^2] \\ &\quad\times(1 + \gamma_1|\psi_{k,n}|^2) - \dot{\psi}_{k,1}^*\psi_{k,2}.\end{aligned} \tag{19}$$

The first terms in the final expressions in Eqs. (18) and (19) are obviously pure imaginary. Substituting Eqs. (18) and (19) into Eq. (17) and using Eqs. (6) and (7), we find

$$\begin{aligned}\frac{d}{dt}E &= -2\mathrm{Re}[\psi_{1,0}^*(s_2\dot{\psi}_{2,1} + s_3\dot{\psi}_{3,1}) + \dot{\psi}_{1,0}^*(s_2\psi_{2,1} + s_3\psi_{3,1}) \\ &\quad + \psi_{1,-1}^*\dot{\psi}_{1,0} + \dot{\psi}_{2,1}^*\psi_{2,2} + \dot{\psi}_{3,1}^*\psi_{3,2}] \\ &= 2\mathrm{Re}\left[\frac{1}{i}(1 + \gamma_1|\psi_{1,0}|^2)(|\psi_{1,-1}|^2 - |s_2\psi_{2,1} + s_3\psi_{3,1}|^2)\right. \\ &\quad \left. + \frac{1}{i}\sum_{k=1}^{3}(1+\gamma_k|\psi_{k,1}|^2)\left(s_k^2|\psi_{1,0}|^2 - |\psi_{k,2}|^2\right)\right] = 0.\end{aligned} \tag{20}$$

The last equality comes from the pure imaginary nature of the expression in square brackets. Equation (20) is nothing but the energy conservation.

Thus we have proved that the norm and energy are conserved for any choice of values s_2 and s_3. In general, however, other conservation rules do not hold. In the next sections we reveal a special case with appropriate choice of s_2 and s_3 which guarantees an infinite number of conservation laws.

III. COMPLETELY INTEGRABLE CASE

A. Dynamics near branching point and sum rule

Among many possible choices of s_2 and s_3, there is one special case in which an infinite number of constants of motion can be found and the DNLSE in the form of an AL equation on a PSG becomes completely integrable. To investigate this case, we first add to each bond B_k $(k = 1,2,3)$ a ghost-bond counterpart B_k' so that $B_k + B_k'$ constitutes an ideal 1D chain (see Fig. 2). Then we suppose that the soliton solution of the AL equation on a PSG is given by

$$\psi_{k,n}(t) = \frac{1}{\sqrt{\gamma_k}} q_{k,n}(t), \quad k = 1,2,3, \tag{21}$$

where $q_{k,n}(t)$ are soliton solutions of the DNLSE with unit nonlinearity on the ideal 1D chain ([24,27,28]):

$$i\dot{q}_n + (q_{n+1} + q_{n-1})(1 + |q_n|^2) = 0, \tag{22}$$

with n being integers in $(-\infty, +\infty)$. The solutions of Eq. (22) may be different among three fictitious chains $B_k + B_k'$ $(k = 1,2,3)$.

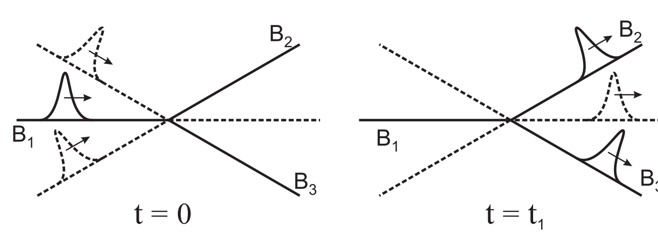

FIG. 2. Real bonds and real solitons (solid lines) and ghost bonds and ghost solitons (broken lines).

Comparing Eqs. (6), (7), and (22), one can find at the vertex the following two equalities:

$$\frac{1}{\sqrt{\gamma_1}}q_{1,1}(t) = \frac{s_2}{\sqrt{\gamma_2}}q_{2,1}(t) + \frac{s_3}{\sqrt{\gamma_3}}q_{3,1}(t), \tag{23}$$

$$\frac{1}{\sqrt{\gamma_k}}q_{k,0}(t) = \frac{s_k}{\sqrt{\gamma_1}}q_{1,0}(t),\ \ k = 2,3. \tag{24}$$

Noting the spatiotemporal behavior of soliton solutions and to guarantee the equality in Eq. (24), $q_{k,n}(t) = s_k\sqrt{\frac{\gamma_k}{\gamma_1}}q_{1,n}(t)$ with $k = 2,3$ should be satisfied for any time t and for any integer n. Hence we obtain

$$s_k\sqrt{\frac{\gamma_k}{\gamma_1}} = 1 \quad \text{or} \quad s_k = \sqrt{\frac{\gamma_1}{\gamma_k}} \quad (k = 2,3) \tag{25}$$

and

$$q_{k,n}(t) \equiv q_n(t), \tag{26}$$

namely, the solution $q_{k,n}(t)$ should be bond independent. With use of Eqs. (25) and (26) in Eq. (23), we have the sum rule among nonlinearity coefficients γ_1, γ_2, and γ_3:

$$\frac{1}{\gamma_1} = \frac{1}{\gamma_2} + \frac{1}{\gamma_3}. \tag{27}$$

Equations (25)–(27) are the necessary and sufficient conditions to see Eqs. (23) and (24). Thus, under the sum rule for nonlinearity coefficients in Eq. (27), the solution on a PSG is given by a common (bond-independent) soliton solution of Eq. (22) multiplied by the square root of the inverse nonlinearity coefficient. For example, the soliton incoming through the bond B_1 is expected to smoothly bifurcate at the vertex and propagate through the bonds B_2 and B_3, as we see in Fig. 4. In the case that γ_1, γ_2, and γ_3 break the sum rule, we see a completely different nonlinear dynamics of solitons such as their reflection and emergence of radiation at the vertex, as shown in Fig. 6. The initial value problem for such a case is outside the scope of the present work.

We also note that the parameters s_2 and s_3 would correspond to $\frac{\alpha_2}{\alpha_1}$ and $\frac{\alpha_3}{\alpha_1}$, respectively, in the previous work [25], although the derivations of the connection formula at the vertex are quite different between the continuum and discrete systems. In fact, s_2 and s_3 are introduced to define the intersite interaction at the vertex and are not obtained from the norm and energy conservations, in contrast to the case of networks consisting of continuum segments [25].

B. An infinite number of constants of motion

It is well known that AL equation on the 1D chain has an infinite number of constants of motion. Now we proceed to obtain an infinite number of constants of motion for general solutions of the AL equation on a PSG. First of all, it should be noted that the solution on a PSG can now be written as

$$\psi_k(t) = \frac{1}{\sqrt{\gamma_k}}\{q_n(t)|n \in B_k\}, \quad k = 1,2,3, \tag{28}$$

where $q(t)$ stands for a general solution of AL equation (22) and is restricted to each bond B_k ($k = 1,2,3$).

While we already proved the conservation of energy, we can generalize it to the general case: Without taking the complex conjugate, Eq. (3) can be explicitly written as

$$Z = -\sum_{n=-1}^{-\infty}\psi_{1,n}^*\psi_{1,n+1} - \sum_{k=2}^{3}\sum_{n=1}^{+\infty}\psi_{k,n}^*\psi_{k,n+1} - \psi_{1,0}^*(s_2\psi_{2,1} + s_3\psi_{3,1}). \tag{29}$$

Substituting Eq. (28) into Eq. (29), Z is rewritten as

$$Z = -\frac{1}{\gamma_1}\sum_{n=0}^{-\infty}q_n^*q_{n+1} - \sum_{k=2}^{3}\frac{1}{\gamma_k}\sum_{n=1}^{+\infty}q_n^*q_{n+1} + \frac{1}{\gamma_1}q_0^*q_1 - \sum_{k=2}^{3}\frac{s_k}{\sqrt{\gamma_1\gamma_k}}q_0^*q_1. \tag{30}$$

Using the value s_k in Eq. (25) and the sum rule in Eqs. (27) and (30) reduces to the constant for the ideal 1D chain [27,28]:

$$Z = -\frac{1}{\gamma_1}\sum_{-\infty}^{+\infty}q_n^*q_{n+1}. \tag{31}$$

Therefore Z in Eq. (29) is a constant of motion, and its real and imaginary parts imply the energy and current, respectively.

For other higher-order conservation rules, we can write them as

$$\frac{1}{\gamma_1}C_m = \frac{1}{\gamma_1}\sum_{n=0}^{-\infty}f_m^{(n)}(\{q_n|n \in B_1\}) + \sum_{k=2}^{3}\frac{1}{\gamma_k}\sum_{n=1}^{+\infty}f_m^{(n)}(\{q_n|n \in B_k\}), \tag{32}$$

with f_m defined as expansion coefficients of the expression (see Ref. [28])

$$\log\left(g_n^{(0)} + g_n^{(1)}z^2 + g_n^{(2)}z^4 + \cdots\right) = f_1^{(n)}z^2 + f_2^{(n)}z^4 + \cdots, \tag{33}$$

where $g_n^{(m)}$ are given by

$$g_n^{(0)} = 1, \quad g_n^{(1)} = R_{n-1}Q_{n-2},$$
$$g_n^{(m)} = \frac{R_{n-1}}{R_{n-2}}g_{n-1}^{(m-1)} - \sum_{l=1}^{m-1}g_{n-1}^{(m-l)}g_n^{(l)}, \quad m = 2,3,4,\ldots, \tag{34}$$

$$R_n = q_{n+2}^*, \quad Q_n = -q_{n+2}. \tag{35}$$

The relations (34) and (35) are obtained by solving Eq. (4.15) in [28], i.e.,

$$g_{n+1}(g_{n+2} - 1) - z^2\frac{R_{n+1}}{R_n}(g_{n+1} - 1) = z^2R_{n+1}Q_n, \tag{36}$$

recursively with use of the expansion

$$g_n = g_n^{(0)} + g_n^{(1)}z^2 + g_n^{(2)}z^4 + \cdots. \tag{37}$$

The right-hand side of Eq. (32) includes some undefined field variables in the ghost bond regions which must be defined as

$$\begin{aligned}\psi_{1,n} &= \sqrt{\frac{\gamma_1}{\gamma_2}}\psi_{2,n} + \sqrt{\frac{\gamma_1}{\gamma_3}}\psi_{3,n} \quad \text{with} \quad n \geqslant 1,\\ \psi_{k,n} &= \sqrt{\frac{\gamma_1}{\gamma_k}}\psi_{1,n}, \quad k = 2,3 \quad \text{with} \quad n \leqslant 0.\end{aligned} \tag{38}$$

The conservation laws in Eq. (32) follow from the nature of solutions (28) and the sum rule for nonlinearity coefficients (27).

For $m = 1$ we obtain current and energy conservation laws. At $m \geqslant 2$ we obtain higher-order conservation laws. Some of the higher-order constants of motion are as follows:

$$\begin{aligned}\frac{1}{\gamma_1}C_2 = -\sum_{k=1}^{3}\sum_{n\in B_k}\Big[&\psi^*_{k,n+1}\psi_{k,n-1}(1+\gamma_k|\psi_{k,n}|^2)\\ &+\frac{\gamma_k}{2}\psi^2_{k,n}(\psi^*_{k,n+1})^2\Big],\end{aligned} \tag{39}$$

$$\begin{aligned}\frac{1}{\gamma_1}C_3 = -\sum_{k=1}^{3}\sum_{n\in B_k}\Big\{&\big[\psi^*_{k,n+2}\psi_{k,n-1}(1+\gamma_k|\psi_{k,n+1}|^2)\\ &+\gamma_k\psi^*_{k,n}\psi^*_{k,n+1}\psi^2_{k,n-1} + (\psi^*_{k,n+1})^2\psi_{k,n}\psi_{k,n-1}\big]\\ &\times(1+\gamma_k|\psi_{k,n}|^2) + \frac{\gamma_k^2}{3}\psi^*_{k,n+1}\psi_{k,n}\Big\},\end{aligned} \tag{40}$$

where field variables at lattice sites of the ghost bonds are defined in Eq. (38).

IV. GENERALIZED STAR AND TREE GRAPHS

Now we proceed to explore soliton solutions of the DNLSE in the form of the AL equation on other types of graphs and explore the sum rule and conservation rules for solitons to propagate through these graphs. The above treatment on a PSG is also true for more general star graphs consisting of N semi-infinite bonds connected at a single vertex. In such cases, the initial soliton at an incoming bond B_1 splits into $N-1$ solitons in the remaining bonds, and the extended version of Eq. (27) is

$$\frac{1}{\gamma_1} = \sum_{j=2}^{N}\frac{1}{\gamma_j}. \tag{41}$$

The solution is given by the equations

$$\psi_{k,n}(t) = \frac{1}{\sqrt{\gamma_k}}q_n(t), \tag{42}$$

where $n = 0,-1,-2,\ldots$ for the first bond ($k=1$) and $n = 1,2,3,\ldots$ for other bonds ($2 \leqslant k \leqslant N$); $q_n(t)$ is a soliton solution of Eq. (22). Conservation laws for this graph can be obtained analogously as in the case of a PSG.

Another example of the graph for which the soliton solution of the DNLSE in the form of the AL equation can be obtained analytically is the tree graph in Fig. 3. Now we provide a soliton solution in this case. We denote bonds of the graph as $B_\Lambda = B_{1ij\cdots m}$ and number the lattice sites on these bonds

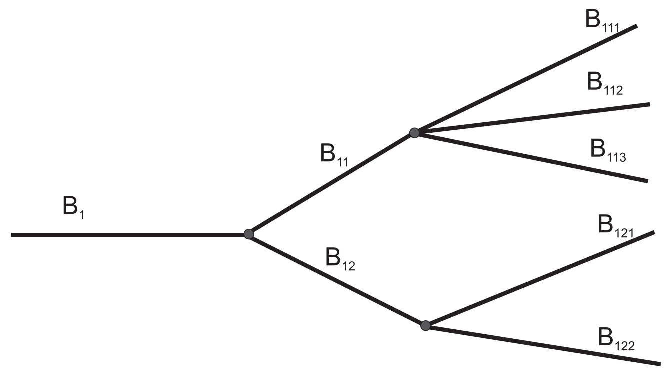

FIG. 3. Tree graph: $B_1 \sim (-\infty,0), B_{11}, B_{12} \sim (0,L)$, and $B_{1ij} \sim (0,+\infty)$ with $i,j = 1,2,\ldots$.

as $1,2,3,\ldots,N_\Lambda$. On each branching point we assume the following conditions hold:

$$\frac{1}{\gamma_\Lambda} = \sum_m \frac{1}{\gamma_{\Lambda m}}. \tag{43}$$

The solution is given by

$$\psi_{\Lambda,n}(t) = \frac{1}{\sqrt{\gamma_k}}q_{n+s_\Lambda}(t), \quad n \in B_\Lambda. \tag{44}$$

Here s_Λ is the number of lattice sites that the soliton passes through from B_1 to B_Λ. For the tree graph it is defined as

$$\begin{aligned} s_1 = s_{1i} = n_0, \quad s_{1ij} = n_0 + N_{1i},\\ s_\Lambda \equiv s_{1ij\cdots lm} = n_0 + N_{1i} + \cdots + N_{1ij\cdots l}.\end{aligned} \tag{45}$$

Below, applying the induction method we give a proof of conservation laws for soliton solutions of the AL equation on a tree graph. Let us denote the tree graph as G and assume the conservation laws to hold in G: $\sum_{B_\Lambda\in G}\sum_{n\in B_\Lambda} f_n^{(k)}(q_{n+s_\Lambda}(t)) = \text{const}$. Then we construct an enlarged tree graph in the following way: First, we choose the arbitrary point N_Φ in the one of rightmost semi-infinite chains B_Φ as a new branching point. We cut off semi-infinite part of this bond at the point N_Φ and attach M semi-infinite bonds to this point. Namely, the bond B_Φ is now replaced by a finite bond $\tilde{B}_\Phi$ connected with M semi-infinite bonds $B_{\Phi m} = \{1,2,\cdots,N_{\Phi m}\}$, with $m = 1,2,\ldots,M$. For the enlarged tree graph, constants of motion are given by

$$\begin{aligned}&\sum_{B_\Lambda\in G-B_\Phi}\gamma_\Lambda^{-1}\sum_{n\in B_\Lambda} f_n^{(k)}(q_{n+s_\Lambda}(t)) + \gamma_\Phi^{-1}\sum_{n\in\tilde{B}_\Phi} f_n^{(k)}(q_{n+s_\Phi}(t))\\ &\quad+\sum_{m=1}^{M}\gamma_{\Phi m}^{-1}\sum_{n\in B_{\Phi m}} f_n^{(k)}(q_{n+s_\Phi+N_\Phi}(t))\\ &=\sum_{B_\Lambda\in G-B_\Phi}\gamma_\Lambda^{-1}\sum_{n\in B_\Lambda} f_n^{(k)}(q_{n+s_\Lambda}(t)) + \gamma_\Phi^{-1}\sum_{n=1}^{N_\Phi} f_n^{(k)}(q_{n+s_\Phi}(t))\\ &\quad+\sum_{m=1}^{M}\gamma_{\Phi m}^{-1}\sum_{n=1+N_{\Phi m}}^{+\infty} f_n^{(k)}(q_{n+s_\Phi+N_\Phi}(t))\\ &= -\left(\gamma_\Phi^{-1} - \sum_{m=1}^{M}\gamma_{\Phi m}^{-1}\right)\sum_{n=1+N_{\Phi m}}^{+\infty} f_n^{(k)}(q_{n+s_\Phi+N_\Phi}(t)) + \text{const.}\end{aligned} \tag{46}$$

It is clear that the final expression becomes constant under the sum rule (43). Thus, starting from the PSG in Fig. 1 and repeating the above procedure, we can get the conservation rule for all tree graphs.

V. TRANSMISSION PROBABILITIES AGAINST INJECTION OF A SINGLE SOLITON

A relevant issue of the above discoveries is the transmission probability against injection of a single soliton. Here we calculate transmission probabilities for a single soliton which is incoming through a semi-infinite bond B_1 and outgoing through the other semi-infinite bonds $\{B_l|l \neq 1\}$.

A single (bright) soliton on a graph, which takes the general form as in Eqs. (28), (42), and (44), is described with use of an AL soliton with $\gamma = 1$ [27]: $\psi_{l,n}(t)$ lying on individual bonds B_l is given by

$$\psi_{l,n}(t) = \gamma_l^{-1/2} \sinh\beta \operatorname{sech}[\beta(n - n_0 - vt)] \times e^{-i(\omega t + \alpha n + \phi_0)}, \quad n \in B_l,\ l = 1,2,3,\ldots,N, \tag{47}$$

where $\omega = -2\cosh\beta\cos\alpha$, $v = -(2/\beta)\sinh\beta\sin\alpha$, $-\pi \leqslant \alpha \leqslant \pi$, $0 < \beta < \infty$, $0 \leqslant \phi_0 < 2\pi$, and n_0 are bond-independent parameters characterizing frequency, velocity, wave number, inverse width of the soliton, initial phase, and initial center of mass, respectively. Equation (47) indicates that a narrow soliton travels faster than wider ones with the same α.

It should be noted that parameter values are common to each bond, except for $\{\gamma_l\}$. Choosing the simplest network PSG in Fig. 1, we give conservative quantities for the solution in Eq. (47) under the sum rule in Eq. (27). First of all, the norm in Eq. (8) turned out to be reduced to the one for the 1D chain with the nonlinearity constant γ_1 and thereby is given by

$$N = 2\beta/\gamma_1. \tag{48}$$

Equation (48) indicates that a narrow soliton has a larger norm than wider ones. As for the energy (E) and current (J), it is convenient to evaluate the combined quantity Z in Eq. (29) with the use of s_2 and s_3 given by Eq. (25). In fact we have

$$E = -2\mathrm{Re}(Z), \quad J = 2\mathrm{Im}(Z). \tag{49}$$

Substituting Eq. (47) into Eq. (29) and using the sum rule in Eq. (27), one obtains

$$Z = \frac{2}{\gamma_1} e^{-i\alpha} \sinh\beta \tag{50}$$

and

$$E = -\frac{4}{\gamma_1}\cos\alpha\sinh\beta, \quad J = -\frac{4}{\gamma_1}\sin\alpha\sinh\beta. \tag{51}$$

As is seen from Eq. (47), the center of mass of the soliton (CMS) on each bond B_l is located at $n = n_0$ at $t = 0$. However, lattice points on the individual semi-infinite bonds are defined on the limited interval. In particular, on outgoing bonds $\{B_l|l \neq 1\}$, their lattice points n are defined in the interval $(1, +\infty)$. If $n_0 < 0$, therefore, the CMS on $\{B_l|l \neq 1\}$ is initially located outside of the real bonds. In such cases we call the soliton a "ghost soliton." When the CMS belongs to a real bond we use the term "real soliton." In Fig. 2, which corresponds to the PSG in Fig. 1, ghost solitons are plotted with a dashed curve while real ones are plotted with a solid line. The soliton dynamics here is governed by a single characteristic time $\tau \equiv \frac{-n_0}{v}$. While for $0 \leqslant t \leqslant \tau$ the soliton at B_1 is a real one and those at B_2 and B_3 are ghosts, for $\tau \leqslant t$ the soliton at B_1 is a ghost and those at B_2 and B_3 are real. At $t = 0$ with $-n_0 \gg 1$, the soliton lying on the bond B_1 is exclusively responsible for the norm N. On the other hand, at $t \gg 1$, the solitons running through the bonds B_2 and B_3 are exclusively responsible for the norm. Therefore, we can naturally define transmission probabilities at $t \to +\infty$.

In general networks, the transmission probability for an arbitrary semi-infinite bond B_l ($l \neq 1$) at discrete time $\hat{t}$ that

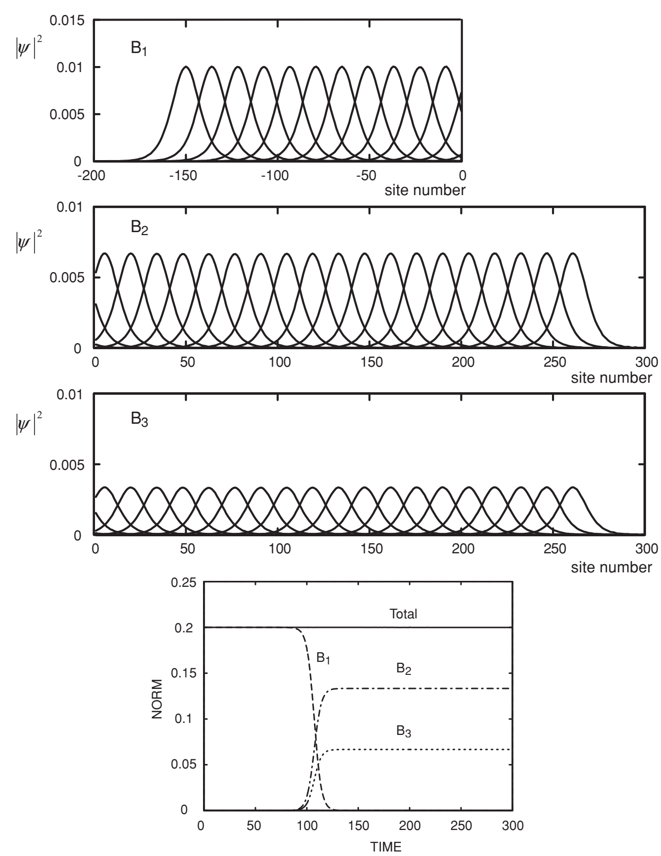

FIG. 4. Numerical result for time evolution of a soliton propagation through a vertex in a PSG. The strengths of nonlinearity at each bond are $\gamma_1 = 1$, $\gamma_2 = 1.5$, and $\gamma_3 = 3$, satisfying the sum rule in Eq. (27). The space distribution of the wave function probability is depicted in every time interval $T = 10.0$ with time used commonly in branches 2 and 3. The abscissa represents discrete lattice coordinates defined in Fig. 1. The initial profile is an Ablowitz-Ladik soliton in Eq. (47) at $t = 0$ with parameters $\beta = 0.1$, $\alpha = 5\pi/4$. The time difference in numerical iteration is $\Delta t = 0.01$. The bottom panel shows the time dependence of partial norms at each of three branches.

makes $v\hat{t}$ integers is defined as

$$\begin{aligned}T_l &= \frac{1}{N\gamma_l}\sum_{n=1}^{+\infty}\ln(1+\gamma_l|\psi_{l,n}|^2)\\ &= \frac{1}{N\gamma_l}\sum_{n=1}^{+\infty}\ln\{1+\sinh^2\beta\,\mathrm{sech}^2[\beta(n-n_0-v\hat{t})]\}\\ &= \frac{\gamma_1}{N\gamma_l}\sum_{n'=1-n_0-v\hat{t}}^{+\infty}\frac{1}{\gamma_1}\ln[1+\sinh^2\beta\,\mathrm{sech}^2(\beta n')].\end{aligned} \quad (52)$$

At $v\hat{t}\to+\infty$, $\sum_{n'=1-n_0-v\hat{t}}^{+\infty}$ on the last line in Eq. (52) tends to $\sum_{n'=-\infty}^{+\infty}$ and this summation gives N, i.e., the normalization of the soliton in the ideal 1D chain with the nonlinearity coefficient γ_1. Therefore,

$$T_l = \frac{\gamma_1}{\gamma_l}. \quad (53)$$

Under the sum rules as in Eqs. (27), (41), and (43), we have the unitarity condition

$$\sum_{l=2}^{N} T_l = 1, \quad (54)$$

where the summation is taken over the semi-infinite bonds except for B_1. The result in Eq. (53) means that the transmission probability is inversely proportional to the strength of nonlinearity in outgoing semi-infinite bonds.

We have checked this result using a numerical simulation of the DNLSE in the form of an AL equation on a PSG in Fig. 1: We numerically iterated Eqs. (2), (6), and (7) with the use of Eq. (25) and chose the initial profile in Eq. (47) with γ_1 and $n_0=-150$ as an incoming soliton. Figure 4 shows the result in the case that the sum rule in Eq. (27) is satisfied: The soliton starting at lattice point $n=-150$ in branch 1 enters the vertex at $n=0$ and is smoothly split into a pair of smaller solitons in branches 2 and 3 with no reflection at the vertex. The velocity and width of the soliton have the definite value common to all bonds, and the squared peak value of the soliton is inversely proportional to γ_k, which is consistent with the result in Eq. (47). The bottom panel in Fig. 4 shows the time dependence of partial norms at each of three branches. With increasing time, the partial norms at branches 2 and 3 converge to the transmission probabilities in Eq. (53).

In Fig. 5, transmission probabilities T_2 and T_3 are plotted as a function of $\frac{\gamma_1}{\gamma_2}$ in the wider range of γ_1 and γ_2 in the case satisfying the sum rule in Eq. (27). We can confirm the linear law predicted in Eq. (53).

Figure 6 shows the result in the case that the sum rule is broken: $\frac{\gamma_1}{\gamma_2}+\frac{\gamma_1}{\gamma_3}\neq 1$. In this case the soliton starting at lattice point $n=-150$ in branch 1 enters the vertex at $n=0$, but it is accompanied by both reflection and emergence of radiation at the vertex. It is very interesting that the velocity of the self-organized soliton has the definite value common to all bonds. In particular, the reflected soliton at branch 1 has the same magnitude of velocity as that of the incident soliton. With increasing time, the partial norms at branches 1, 2, and 3 would converge to the reflection (on B_1) and transmission probabilities (on B_2 and B_3). For some other choice of γ_1, γ_2, and γ_3 that breaks the sum rule (which is not shown here), the

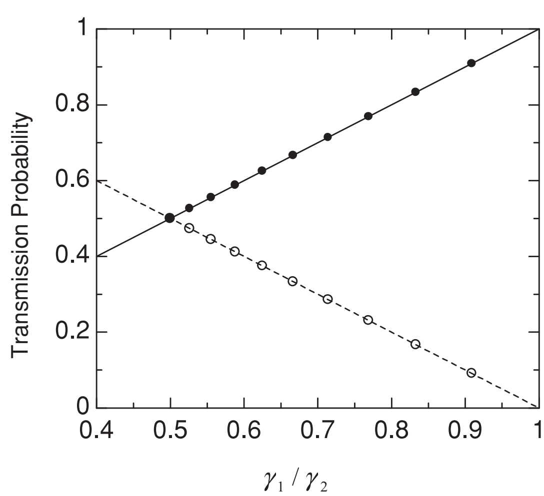

FIG. 5. Transmission probabilities as a function of $\frac{\gamma_1}{\gamma_2}$ in a PSG. Symbols and lines denote numerical and theoretical results, respectively. A solid line with • and a broken line with ○ correspond to T_2 and T_3, respectively.

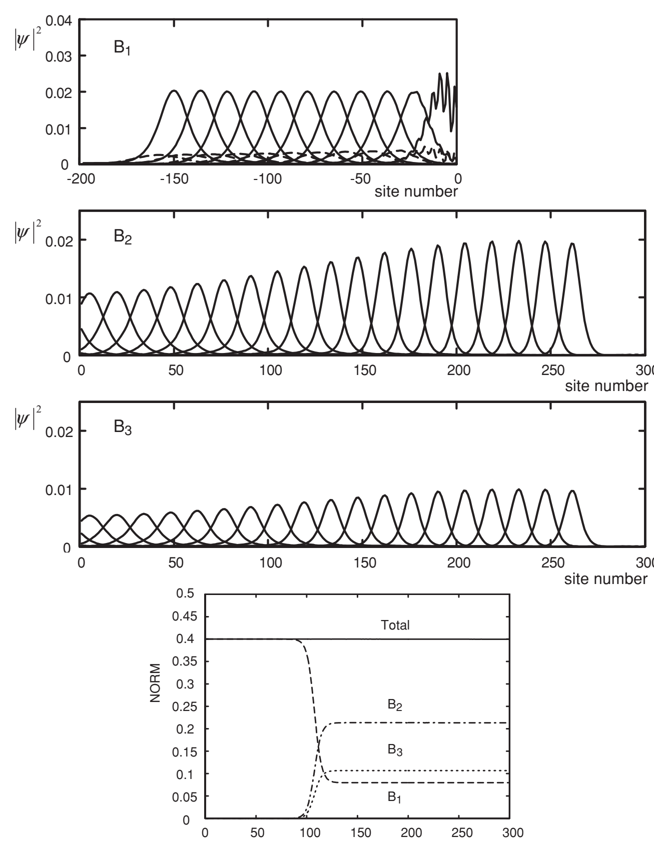

FIG. 6. Numerical result for time evolution of a soliton propagation through a vertex in the case of $\gamma_1=0.5$, $\gamma_2=1.5$, $\gamma_3=3$, which breaks the sum rule. The initial profile and parameter values are the same as in Fig. 4. In the top panel, dashed curves indicate a propagation of the reflected soliton. The bottom panel shows the time dependence of partial norms at each of three branches.

asymptotically ($t \gg 1$) equal velocity of solitons running on all three semi-infinite bonds can also be observed and provides an open question to be resolved in due course.

VI. SUMMARY AND DISCUSSIONS

We have derived conditions under which an AL-type DNLSE on simple networks is mapped to the original one on the ideal 1D chain and becomes completely integrable. Here the strength of cubic nonlinearity is different from bond to bond, and networks are assumed to have at least two semi-infinite bonds with one of them used as an incoming bond. Our findings are that (1) the solution on each bond is a part of the universal (bond-independent) soliton solution of the completely integrable DNLSE on the 1D chain, but it is multiplied by the inverse of the square root of bond-dependent nonlinearity; (2) the inverse nonlinearity at an incoming bond should be equal to the sum of inverse nonlinearities at the remaining outgoing bonds; and (3) with use of the above two findings, there exist an infinite number of constants of motion. The parameters s_2 and s_3, which played an essential role in deriving the connection formula, are introduced to define the intersite interaction at the vertex and are not obtained from the norm and energy conservations, in marked contrast to the case of networks consisting of continuum segments [25]. The argument on a branched chain or a PSG is generalized to general star graphs and tree graphs by using the induction method. As a practical issue, with the use of an AL soliton injected through the incoming bond, we obtain transmission probabilities inversely proportional to the strength of nonlinearity on the outgoing bonds.

ACKNOWLEDGMENT

K.N. is grateful to F. Abdullaev for suggesting the significance of extending our preceding work on the continuum NLSE to the discrete case.

[1] Y. S. Kivshar and G. P. Agarwal, *Optical Solitons: From Fibers to Photonic Crystals* (Academic Press, San Diego, CA, 2003).
[2] L. V. Yakushevich, A. V. Savin, and L. I. Manevitch, Phys. Rev. E **66**, 016614 (2002).
[3] F. S. Cataliotti, S. Burger, C. Fort, P. Maddaloni, F. Minardi, A. Trombettoni, A. Smerzi, and M. Inguscio, Science **293**, 843 (2001).
[4] I. N. de Oliveira, F. A. B. F. de Moura, M. L. Lyra, J. S. Andrade Jr., and E. L. Albuquerque, Phys. Rev. E **81**, 030104(R) (2010).
[5] F. Corson, Phys. Rev. Lett. **104**, 048703 (2010).
[6] E. Katifori, G. J. Szollosi, and M. O. Magnasco, Phys. Rev. Lett. **104**, 048704 (2010).
[7] P. Exner and P. Šeba, Phys. Lett. **128A**, 493 (1988).
[8] P. Exner and P. Šeba, Rep. Math. Phys. **28**, 7 (1989).
[9] T. Kottos and U. Smilansky, Ann. Phys. (NY) **274**, 76 (1999); S. Gnutzmann and U. Smilansky, Adv. Phys. **55**, 527 (2006).
[10] P. Kurasov and F. Stenberg, J. Phys. A **35**, 101 (2002); P. Kurasov and M. Nowaczyk, *ibid.* **38**, 4901 (2005).
[11] P. Kuchment and O. Post, Commun. Math. Phys. **275**, 805 (2007).
[12] P. Exner, J. P. Keating, P. Kuchment, and T. Sunada, *Analysis on Graphs and Its Applications* (American Mathematical Society, Providence, RI, 2008).
[13] S. Gnutzmann, U. Smilansky, and S. Derevyanko, Phys. Rev. A **83**, 033831 (2011).
[14] R. Adami, C. Cacciapuoti, D. Finco, and D. Noja, Rev. Math. Phys. **23**, 409 (2011).
[15] S. Flach and C. R. Willis, Phys. Rep. **295**, 181 (1998).
[16] R. Burioni, D. Cassi, P. Sodano, A. Trombettoni, and A. Vezzani, Chaos **15**, 043501 (2005); Physica D **216**, 71 (2006).
[17] A. S. Pikovsky and D. L. Shepelyansky, Phys. Rev. Lett. **100**, 094101 (2008).
[18] G. Kopidakis, S. Komineas, S. Flach, and S. Aubry, Phys. Rev. Lett. **100**, 084103 (2008).
[19] M. J. Ablowitz and H. Segur, J. Math. Phys. **16**, 1054 (1975).
[20] A. S. Fokas, A. R. Its, and L.-Y. Sung, Nonlinearity **18**, 1771 (2005).
[21] J. I. Ramos and F. R. Villatoro, Math. Comput. Modell. **20**, 31 (1994).
[22] A. S. Fokas and A. R. Its, J. Phys. A **37**, 6091 (2004).
[23] C. Sulem and P. L. Sulem, *The Nonlinear Schrödinger Equation* (Springer, New York, 1999).
[24] M. J. Ablowitz, B. Prinari, and A. D. Trubatch, *Discrete and Continuous Nonlinear Schrödinger Systems* (Cambridge University Press, Cambridge, UK, 2004).
[25] Z. Sobirov, D. Matrasulov, K. Sabirov, S. Sawada, and K. Nakamura, Phys. Rev. E **81**, 066602 (2010).
[26] V. B. Zakharov and A. B. Shabat, Sov. Phys. JETP **34**, 62 (1972).
[27] M. J. Ablowitz and J. F. Ladik, J. Math. Phys. **16**, 598 (1975).
[28] M. J. Ablowitz and J. F. Ladik, J. Math. Phys. **17**, 1011 (1976).
[29] G. Biondini and G. Hwang, Inverse Probl. **24**, 065011 (2008).
[30] A. B. Aceves, C. De Angelis, T. Peschel, R. Muschall, F. Lederer, S. Trillo, and S. Wabnitz, Phys. Rev. E **53**, 1172 (1996).
[31] S. Yomosa, J. Phys. Soc. Jpn. **52**, 1866 (1983).
[32] S. Kivshar and B. A. Malomed, Rev. Mod. Phys. **63**, 761 (1989).
[33] S. Takeno, J. Phys. Soc. Jpn. **61**, 1433 (1992).
[34] V. V. Konotop and S. Takeno, Phys. Rev. B **55**, 11342 (1997).
[35] M. Toda, Phys. Rep. **18**, 1 (1975); *Theory of Nonlinear Lattices* (Springer, Berlin, 1981).